A New Global Land-Use and Land-Cover Change Product at a 1-km Resolution for 2010 to 2100 Based on Human–Environment Interactions

Xia Li, Guangzhao Chen, Xiaoping Liu, Xun Liang, Shaojian Wang, Yimin Chen, Fengsong Pei & Xiaocong Xu

Published online: 27 Apr 2017.

Submit your article to this journal ↗

View related articles ↗

View Crossmark data ↗

A New Global Land-Use and Land-Cover Change Product at a 1-km Resolution for 2010 to 2100 Based on Human–Environment Interactions

Xia Li ⬤,* Guangzhao Chen,* Xiaoping Liu ⬤,* Xun Liang,* Shaojian Wang,* Yimin Chen,* Fengsong Pei,[†] and Xiaocong Xu*

*School of Geography and Planning, Sun Yat-sen University
[†]School of Geography, Geomatics, and Planning, Jiangsu Normal University

Global land-use and land-cover change (LUCC) data are crucial for modeling a wide range of environmental conditions. So far, access to high-resolution LUCC products at a global scale for public use is difficult because of data and technical issues. This article presents a Future Land-Use Simulation (FLUS) system to simulate global LUCC in relation to human–environment interactions, which is built and verified by using remote sensing data. IMAGE has been widely used in environmental studies despite its relatively coarse spatial resolution of 30 arc-min, which is about 55 km at the equator. Recently, an improved model has been developed to simulate global LUCC with a 5-min resolution (about 10 km at the equator). We found that even the 10-km resolution, however, still produced major distortions in land-use patterns, leading urban land areas to be underestimated by 19.77 percent at the global scale and global land change relating to urban growth to be underestimated by 60 to 97 percent, compared with the 1-km resolution model proposed through this article. These distortions occurred because a large percentage of small areas of urban land was merged into other land-use classes. During land-use change simulation, a majority of small urban clusters were also lost using the IMAGE product. Responding to these deficiencies, the 1-km FLUS product developed in this study is able to provide the spatial detail necessary to identify spatial heterogeneous land-use patterns at a global scale. We argue that this new global land-use product has strong potential in radically reducing uncertainty in global environmental modeling. *Key Words: cellular automaton, FLUS, global land use change, IMAGE, 1-km resolution.*

全球土地使用与土地覆盖变迁 (LUCC) 数据, 对模式化大规模环境状态而言相当关键。至今, 由于数据与技术问题, 取得高分辨率的全球尺度 LUCC 产品以作为公共使用仍然是困难的。本文呈现未来土地使用模拟 (FLUS) 系统, 以模拟全球 LUCC 之于人类—环境的互动, 该系统透过使用遥感数据建立并进行证实。尽管 IMAGE 相对而言粗糙的空间分辨率为三十弧分, 在赤道上大约为五十五公里, 但它仍在环境研究中受到广泛使用。晚近则发展出改良的模式, 以五弧分的分辨率 (在赤道上约为十公里) 模拟全球 LUCC。我们发现, 即便是十公里的分辨率, 仍然产生了土地使用模式的重大扭曲, 并且相较于本文所提出的一公里分辨率模型而言, 导致了全球尺度的城市土地面积被低估了百分之十九点七七, 而关乎城市成长的全球土地变迁, 则被低估了百分之六十到九十七。这些扭曲因大幅比例的城市土地小型面积合并到其他土地使用类别而发生。在土地使用变迁模拟中, 运用 IMAGE 产品亦遗漏了大部份的小型城市集群。回应上述缺点, 本研究所建立的一公里 FLUS 产品, 能够提供指认全球尺度空间异质的土地使用模式所需的空间细节。我们主张, 此一崭新的全球土地使用产品, 具有强大的潜力大幅降低全球环境模式化中的不确定性。 关键词: 细胞自动机, FLUS, 全球土地使用变迁, IMAGE, 一公里分辨率。

Los datos sobre cambios del uso del suelo y de cobertura de la tierra (LUCC) a nivel global son cruciales para modelar una amplia gama de condiciones ambientales. Hasta ahora, el acceso a productos de los LUCC a escala global para uso público es difícil debido a problemas técnicos y de datos. Este artículo presenta un sistema de Simulación de Uso Futuro del Suelo (FLUS) para simular los LUCC globales en relación con las interacciones humano–ambientales, el cual está construido y verificado mediante el uso de datos originados por percepción remota. El IMAGE ha sido ampliamente utilizado en estudios ambientales a pesar de su resolución espacial relativamente ruda de 30 minutos de arco, que es de alrededor de 55 km sobre el ecuador. Recientemente, se ha desarrollado un modelo mejorado para simular los LUCC globales con una resolución de 5-minutos (alrededor de 10 km en el ecuador). Sin embargo, hallamos que incluso la resolución de 10-km sigue produciendo distorsiones importantes en los patrones de uso del suelo, lo cual conduce a la subestimación de las áreas de suelo urbano en un 19.77 por ciento en la escala global y a que el cambio global de la tierra relacionado con el crecimiento urbano se subestime entre un 60 a un 97 por ciento, comparado con el modelo de 1-km de resolución

propuesto en este artículo. Estas distorsiones ocurrieron debido a que un porcentaje grande de áreas pequeñas de tierra urbana se consolidaron con otros tipos de usos del suelo. Durante la simulación del cambio de uso del suelo usando el producto IMAGE también se perdieron una mayoría de los pequeños agrupamientos urbanos. Respondiendo a estas deficiencias, el producto FLUS de 1-km desarrollado en este estudio tiene la capacidad de proveer el detalle espacial que se necesita para identificar los patrones espaciales de usos heterogéneos del suelo a escala global. Sostenemos que este nuevo producto para calcular el uso del suelo global tiene fuerte potencial para reducir radicalmente la incertidumbre en el modelado ambiental global. *Palabras clave: Palabras clave: autómata celular, FLUS, cambio global del uso del suelo, IMAGE, resolución de 1-km.*

Human activities have contributed to major land-use and land-cover change (LUCC) at both regional and global scales. In the land-use system, small percentage changes in the extent of urban areas can substantially alter climate, biogeochemistry, and hydrology at local, regional, and global scales (Atkinson 2000; Schneider, Friedl, and Potere 2009). The alterations brought about by such changes affect surface energy budgets, hydrological cycles, and biogeochemical cycles relating to carbon and nitrogen (Seto and Shepherd 2009). Land-use changes, especially those that take the form of urban expansion, will continue to exert great impacts on ecological resources and processes well into the future as rapid economic and population growth continues apace in many developing countries. As a result, changing landscape patterns can be expected to alter the processes and functions of natural ecosystems at scales extending from the local to the global. Research indicates that such changes not only substantially transform landscapes but also greatly influence the biogeochemical cycle and photosynthetic productivity of terrestrial ecosystems (Gregg, Jones, and Dawson 2003).

Mapping current and historical land-use activity patterns provides an important basis against which the consequences of anthropogenic changes to the Earth's surface can be assessed over time (Hurtt et al. 2006). Similarly, the simulation of future land-use changes can provide equally crucial information, albeit with respect to a future condition, supporting the evaluation of the impacts and effectiveness of land-use planning and policy under various possible future conditions. Such scenario-based simulation has become a useful support for analyzing potential land-use change in an uncertain future (Sohl et al. 2012). Land-use change models are now, in fact, considered to be central in the global-scale assessment of a series of important issues, such as biodiversity, water cycles, and climate adaptation and mitigation policies (Meiyappan et al. 2014). For example, future land-use change estimates constitute important inputs for carbon-climate projections (Hurtt et al. 2011), which can in turn be used to assess the consequences of potential greenhouse gas (GHG) emissions and predict prospective changes in climate (Sleeter et al. 2012).

The spatially explicit allocation of land-use change to a grid cell involves a complex process that must pinpoint the relationships between land-use change and its driving forces. Studies have shown that a variety of physical and economic factors can be treated as the drivers for modeling land-use dynamics (Letourneau, Verburg, and Stehfest 2012; Seto, Güneralp, and Hutyra 2012). Existing literature has demonstrated that cellular automata constitute a suitable paradigm in representing complex land-use dynamics by avoiding the use of tedious mathematical equations (Batty and Xie 1994; Clarke, Hoppen, and Gaydos 1997; Li and Yeh 2000, 2002; Santé et al. 2010). A number of past studies have deployed sophisticated techniques such as logistic regression and data mining to quantify the relations between land-use change and its driving forces (Wu 2002; Li and Yeh 2004).

Land-use change models have rather been designed for studies at local or regional scales (Meiyappan et al. 2014). Examples of regional-scale land-use simulation based on the cellular automata techniques include the simulation of land-use changes in the Pearl River Delta, in the San Francisco and Washington/Baltimore region, and in the Amazon basin (Clarke and Gaydos 1998; Li and Yeh 2000; Soares-Filho et al. 2006; Liu et al. 2008).

There are very limited global-scale modeling approaches because they are simply too difficult to implement, despite the fact that global-scale land-use modeling is required in many situations (Meiyappan et al. 2014). The limited global land-change models that do exist are unable to satisfy current needs, as they produce global land-use products at coarse resolutions due to very high demands on computing power for continental or global analysis (Schaldach et al. 2011).

A major challenge for the field of global environmental change studies thus lies in im'proving existing coarse-scale global assessments by achieving finer

spatial details. Many global studies are based on projections of land use and land cover for a relatively small number of regions or using a relatively coarse resolution of spatial grids (Sleeter et al. 2012). Because high-resolution land-use change products are unavailable at the global scale, an approximation method has to be adopted whereby the dominant land cover is represented within a grid—for example, at 30 arc-min (approximately 55 km at the equator) resolution (Verburg et al. 2013). Recently, a new land-use product of 30-m resolution derived from the NASA Landsat TM/ETM satellite images was made available but only for two years, 2000 and 2010 (J. Chen et al. 2015). Land-use information at a finer scale for future years is still unavailable. The coarseness of existing analysis has constrained the value of using these global simulation models. Efforts have thus been made to develop models to downscale the projections of future LUCC at smaller spatial resolutions and more detailed thematic resolutions.

Among the very limited number of global-scale simulation models that exist today that are available for public use, the IMAGE module is the most well known (Letourneau, Verburg, and Stehfest 2012). IMAGE can spatially allocate crops, pasture, and bioenergy using an agroeconomic method. The land-use allocation considers a range of factors, including climate and climate variability, soil and terrain characteristics, and socioeconomic variables like population density and accessibility. This model is able to allocate agricultural land use to grid cells in an iterative process until the required regional production of crops and grass is met. The projected land-cover types are modeled to a grid at 30 arc-min resolution based on decision rules that consider a series of potential crop and grass yields, and suitability factors (Zuidema et al. 1994).

Most global land-use change models, including those using IMAGE, represent land-use patterns at a coarse resolution of 30 arc-min (approximately 55 km at the equator). In the past three decades, efforts have been made to develop more advanced simulation models for predicting urban and land-use dynamics—these, however, have generally been applicable to small regions or countries (Batty and Xie 1994; Clarke, Hoppen, and Gaydos 1997; Li and Yeh 2000; Wu 2002; Santé et al. 2010; Li, Chen, et al. 2011; Liu et al. 2014). Several new models have been proposed in recent years that are suitable for global land-use simulation; however, these are mainly able to represent LUCC at resolutions ranging between 5 and 30 arc-min (Letourneau, Verburg, and Stehfest 2012). Major improvements have been made through the development of the LUSs model (Letourneau, Verburg, and Stehfest 2012) and the CLUMondo model (van Asselen and Verburg 2013), which can both simulate global-scale land change with a finer resolution of 5 arc-min (approximately 10 km at the equator). Simulation results, however, have not as yet been made available for public use for either of these models. The 30-min IMAGE product provides the finest resolution available for public use (Meiyappan et al. 2014). The problem with even this resolution is that pixels within the model represent only dominant land-cover types, thereby ignoring a great deal of landscape heterogeneity. An example of such simplification can be found in the study by Hurtt et al. (2011) wherein the authors presented a method to model global, gridded, crop, pasture, ice and water, and urban land area annually for the time period from 1500 to 2100 at a resolution of 30 min. This resolution reduces land-use patterns to the dominant land-cover/land-use type, resulting in the loss of landscape heterogeneity (Letourneau, Verburg, and Stehfest 2012). Without being able to account for enough spatial heterogeneity, scholars face problematic levels of uncertainty in undertaking impact assessments (Verburg et al. 2013).

Time-series land-use products of fine resolution can help us to better assess land changes and environmental impacts. For example, assessment of urbanization impact on carbon sequestration and land degradation is highly dependent on fine resolution products (Verburg et al. 2006) as these products provide detailed information about the composition of landscapes (van Asselen and Verburg 2013). It is considered that the recent development of 5 arc-min resolution of global land products is a trade-off between the 1-km grid and the 0.5° grid (Schaldach et al. 2011). So far the 1-km grid is used for only the European scale analysis by Verburg et al. (2006) because of very high demands on computing power for continental or global analysis. Their coarse resolutions will compromise the spatial detail of land-use change patterns, particularly in smaller countries (Schaldach et al. 2011).

Besides the coarseness of their spatial resolution, existing approaches have a tendency to disregard urban conditions (Sohl et al. 2012). Many existing models are unable to deal with urban development, although the models provide estimates for major land-use and land-cover (LULC) types, such as agricultural and natural vegetation classes. Missing urban change information can severely hamper the use of these products in land-use modeling. Urban development contributes to

the most important types of land-use changes and has a profound impact on ecological systems (Schneider, Friedl, and Potere 2009; Seto and Shepherd 2009). The objective of the study detailed in this article was to create the first global LUCC product able to operate at a 1-km resolution, to incorporate urban dynamics as a factor, and to preserve spatial details in representing land-use patterns. Targeted at public use, this study also presents a new global land-use simulation model (Future Land-Use Simulation; FLUS) as well as finer resolution land-use change data.

Method

In this article, we propose an integrated approach in order to refine the resolution of global land-use change products, by producing a 1-km resolution product that is able to provide greater spatial detail with respect to land-use patterns. This model consists of two linked components: one that encompasses "top-down" economic modeling using IMAGE and a "bottom-up" spatial modeling component using cellular automata (CA). In our design, the aggregated LULC information from the IMAGE module is used to generate constraints for the next step of spatial modeling.

In the integrated approach followed in this article, two primary modules are integrated to facilitate global LUCC modeling at a fine resolution (Figure 1). First, IMAGE is used to obtain projected aggregated amounts for each land-use type for seventeen world regions (Sleeter et al. 2012). In reality, land-use changes are driven by a range of different processes, which include population increases and landscape changes caused by climate change. In the IMAGE module, population and macroeconomic drivers play the key role in affecting land-use change. IMAGE provides future LULC information for 30-min grid cells globally, creating the spatial distribution of LULC based on biophysical factors such as climate and soils (Strengers et al. 2004).

Second, we also present a CA-based model—the FLUS model (Liu et al. forthcoming)—for modeling multitype land-use conversion at the global scale by coupling human and natural effects (Figure 1). The FLUS model explicitly simulates the long-term spatial trajectories of multiple LUCC. The climate sector (annual precipitation and temperature) is incorporated, and the mechanism of self-adaptive inertia and competition is adopted in the modeling process (Figure 1).

In this FLUS model, the probability-of-occurrence surfaces for each land-cover type are determined based on the unique biophysical and socioeconomic drivers (Sohl and Sayler 2008). Statistical methods, such as logistic regression, have been employed to map probability-of-occurrence surfaces (van Asselen and Verburg 2013). The conversion between multiple land-use types can be very complex, however—as such, artificial neural networks (ANNs) are more effective for mapping nonlinear relationships (Li and Yeh 2002). We therefore chose to base FLUS on ANNs to simulate the conversion between multiple land-use types. The CA allocation is implemented in two steps: (1) an ANN is used to train and estimate the probability-of-occurrence surfaces of land-use on a specific grid cell, and (2) an elaborated self-adaptive inertia and competition mechanism addresses the competition and interactions among different land-use types.

The self-adaptive inertia and competition mechanism is developed to establish the relationship between local-scale and global-scale dynamics. In this mechanism, a self-adaptive inertia coefficient for each land-use type is defined to autoadjust the inheritance of the current land-uses on each grid cell according to differences between the macro demand (the "desired" aggregated amount from the seventeen regions of the IMAGE model) and allocated amount (the simulated amount at time t) of the land-uses. This coefficient is defined as

$$\text{Inertia}_k^t = \begin{cases} \text{Inertia}_k^{t-1} & \text{if } |D_k^{t-1}| \leq |D_k^{t-2}| \\ \text{Inertia}_k^{t-1} \times \dfrac{D_k^{t-2}}{D_k^{t-1}} & \text{if } D_k^{t-1} < D_k^{t-2} < 0 \\ \text{Inertia}_k^{t-1} \times \dfrac{D_k^{t-1}}{D_k^{t-2}} & \text{if } 0 < D_k^{t-2} < D_k^{t-1} \end{cases},$$

(1)

where Inertia_k^t denotes the inertia coefficient for land-use type k at iteration time t. The D_k^{t-1} denotes the difference between the macro demand and allocated amount of the land-use type k until iteration time $t-1$. Note that the inertia coefficient is defined with respect to the current land type occupying the grid cell. Thus, if the land-use type k to be allocated is not the same as the current land-use type, then the inertia coefficient of land-use type k will be set to 1 and will not alter the total probability of land-use type k for this grid cell.

Through these two steps, the combined probabilities of all land-use types at each specific grid cell are
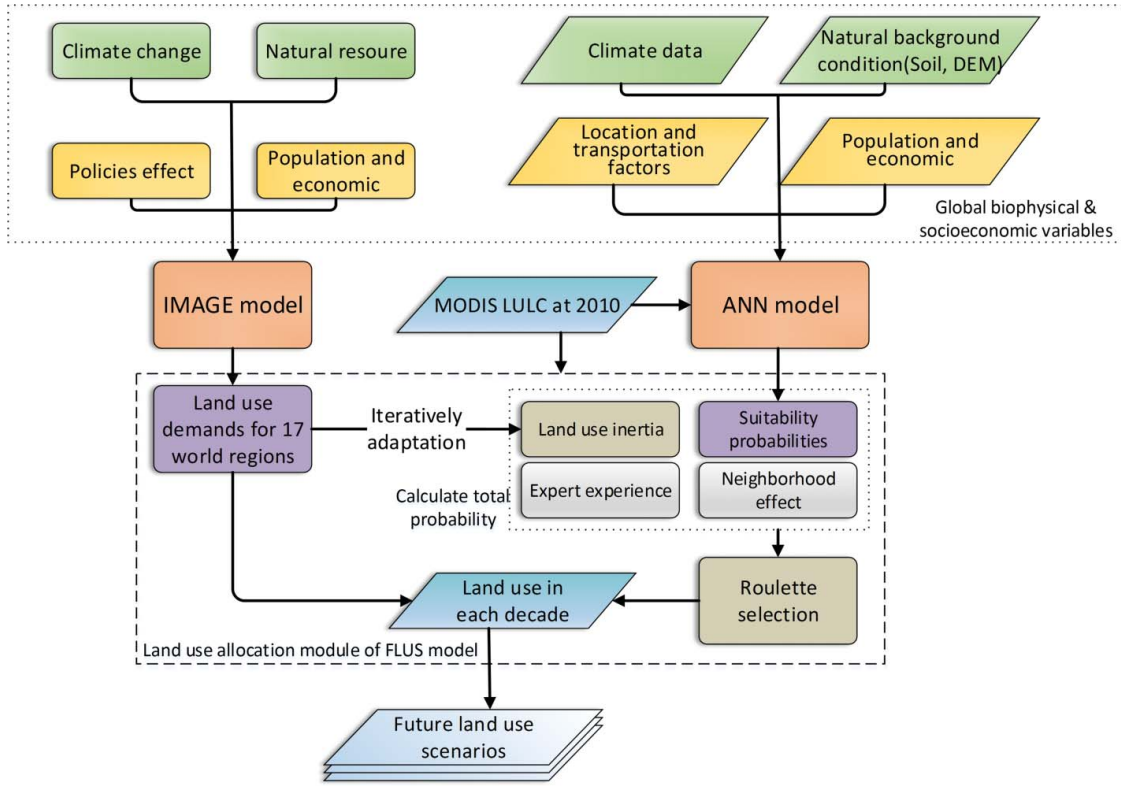
Figure 1. A Future Land-Use Simulation system, coupling human and natural effects for global land-use and land-cover change simulation. *Note*: DEM = digital elevation model; LULC = land use and land cover; ANN = artificial neural network; FLUS = Future Land-Use Simulation. (Color figure available online.)

estimated and the dominant land-use type is allocated to this grid cell during a CA iteration. The combined probabilities are thus calculated according to the following equation:

$$TP^t_{i,k} = P_{i,k} \times \Omega^t_{i,k} \times inertia^t_k \times con_{c \rightarrow k}, \qquad (2)$$

where $TP^t_{i,k}$ denotes the total (combined) probability of the grid cell i to covert from the original land-use into the target one k at iteration time t; $P_{i,k}$ denotes the probability-of-occurrence of land-use type k on grid cell i, which is generated by the ANN algorithm; $\Omega^t_{i,k}$ denotes the neighborhood effect of land-use type k on grid cell i at iteration time t; and $con_{c \rightarrow k}$ refers to a binary conversion constraint from the original land-use type c to the target one k (1 denotes possible conversion and 0 denotes impossible conversion; Figure 2); $Inertia^t_k$ denotes the inertia coefficient of land-use type k at iteration time t. It is a parameter that represents the inheritance of previous land-use types and is automatically adjusted by the self-adaptive inertia and competition mechanism.

After estimating the combined probability for each iteration time, a roulette selection mechanism

is developed to establish the competition relationship between different land-uses and determine whether there is a final change in land-use type on each cell (Figure 3). A roulette selection is designed to reflect this mechanism—a land-use type with a higher combined probability score is more likely to be selected as the target land-use type, but those with relatively lower ones still have some chance to convert (Liu et al. 2010). The objective is to reflect the uncertainty, complexity, and diversity of actual land-use change. This mechanism is important for simulating real-world leapfrog growth and alternate change between different land-uses (Y. Chen et al. 2016).

The implementation of FLUS is facilitated by using the package of GeoSOS-FLUS, which can be downloaded at http://www.geosimulation.cn/flus.html. The FLUS model assumes LUCC allocation to be determined by site-specific characteristics, such as the probability of occurrence. The main inputs to the FLUS include the initial LULC types and spatially explicit biophysical and socioeconomic variables at each grid cell. FLUS is a useful tool for implementing global land-use simulation based on CA techniques.

Figure 2. Constraints for land-use conversion (Schaldach et al. 2011).

Model Implementation and Results

Data and Spatial Variables

The creation of this FLUS product requires the input of an initial LULC map, which formed the starting point for global LUCC simulation. Because global LULC maps are scarce, this initial map was retrieved from the MODIS Land Cover Type Product (MCD12Q1; https://lpdaac.usgs.gov/). IMAGE was just used to obtain the aggregated projected land-use information of seventeen regions. The original resolution of 463 m of the MODIS images was first downgraded to 1 km to obtain the initial land-use information for the simulation. Because of the inconsistency of land-use classes between MODIS and IMAGE, a reclassification scheme was used to merge the initial classes of MODIS in 2010 to six major classes (Table 1), thereby making these two data sets comparable for the purposes of land-use change simulation.

In addition to the initial land-use classes, we formulated a range of spatial variables to represent the driving forces behind land-use dynamics. Table 2 provides information about the format and sources of the spatial variables we chose to integrate into the FLUS system; each of these are commonly used in global land-use simulation
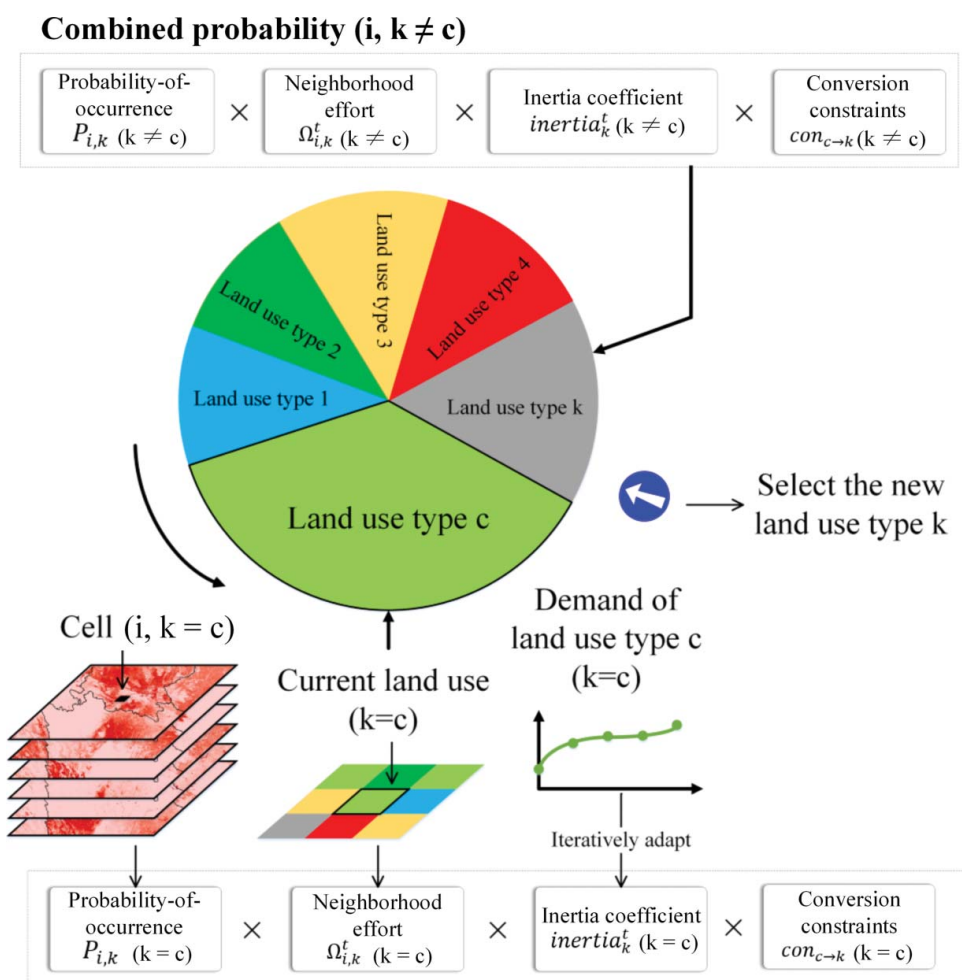

Figure 3. The competition mechanism implemented by a roulette selection procedure. (Color figure available online.)

models (Letourneau, Verburg, and Stehfest 2012; van Asselen and Verburg 2013). These variables must be transformed into the same resolution and projection prior to model implementation. In this study, they were resampled and converted into 1-km grids with the projection *WGS_1984_Cylindrical_Equal_Area*.

IMAGE data usually cannot be used "as is" in applications because of their various limitations (Sohl et al. 2012). A major problem is that IMAGE assumes a frozen (unchanged) urban area in representing land-use dynamics. The fixed urban area of IMAGE should be adjusted according to the population growth rate and a scaling factor (Sleeter et al. 2012). This assumes that the increase in population can be proportionally related to the increase in the amounts of developed lands. The population factor alone, however, cannot reflect the impact of other social and economic factors (e.g., economic growth, technology, and societal attitudes) on the demand for urban land. Some IMAGE scenarios might share the same population projections (e.g., Scenarios A1B and B1). Therefore, we used a scaling factor to reflect the land demand in accordance with the economic and environmental implications of the scenario (Nakicenovic and Swart 2000). As

such, we modified the fixed urban area by considering land development as follows (Sleeter et al. 2012):

$$A(t)^U = A(t-1)^U * (\Delta POP(t) * \sigma), \quad (3)$$

where $A(t)^U$ is the projected amount of urban land (U) for year t, $\Delta POP(t)$ is the projected percent change in population from $t-1$ to t in IMAGE at five-year intervals, and σ is a scaling factor that is used to reflect the land demands from the economic and environmental initiatives of the Intergovernmental Panel on Climate Change Special Report on Emission Scenarios (IPCC SRES) scenarios.

Because the modifications performed on the urban area increase its size, the projected area of other land-use classes from IMAGE must be adjusted accordingly. We regard the missing actual urban growth as an error in the IMAGE product and the missing growth must be deducted from other land-use classes. A simple way is to deduct this amount from the projected areas of other land-use classes proportionally. Urban area expansion dominantly affects agricultural area, though, and an equal spreading across land-use types is not correct.

Table 1. Land-use classes for global land-use and land-cover change simulation based on MODIS and IMAGE classes

This study	MODIS	IMAGE
Water	Water bodies	None
Forest	Evergreen needleleaf forests	Boreal forest
	Evergreen broadleaf forests	Carbon plantations
	Deciduous needleleaf forests	Cool conifer forest
	Deciduous broadleaf forests	Regrowing vegetation (abandoning)
	Mixed forests	Regrowing vegetation (timber)
		Temperate deciduous forest
		Temperate mixed forest
		Tropical forest
		Tropical woodland
		Warm mixed forest
Grassland	Closed shrublands	Scrubland
	Woody savannas	Extensive grassland
	Savannas	Savanna
	Grasslands	Grassland and steppe
	Permanent wetlands	
Farmland	Croplands	Agricultural land
	Cropland/natural vegetation mosaics	
Urban	Urban and built-up lands	None
Barren	Open shrublands	Tundra
	Barren or sparsely vegetated	Wooded tundra
	Snow and ice	Hot desert
		Ice

Table 2. Spatial variables retrieved from global data sets for implementing the Future Land-Use Simulation model

Drivers	Year	Resolution	Data sources
Population	2010	0.5′	LandScan 2010 Global Population Project
DEM	2000	0.5′	Hijmans et al. (2005)
Slope	2000	0.5′	Retrieved from DEM
Distance to urban centers(population $> 30 \times 10^3$)	2014	1 km	United Nations, Department of Economic and Social Affairs, Population Division (2014)
Distance to roads	1980–2010	1 km	NASA, Socioeconomic Data and Applications Center, Global Roads Open Access Data Set, version 1
Soil quality (nutrient availability)	2008	5′	Fischer et al. (2008)
Soil quality (oxygen availability to roots)			
Soil quality (excess salts)			
Soil quality (workability)			
Annual mean temperature	2000	0.5′	Hijmans et al. (2005)
Temperature seasonality			
Temperature annual range			
Annual precipitation			
Precipitation seasonality			

Note: DEM = digital elevation model.

We used historical data to obtain the proportion of land loss due to urban encroachment on each land-use class. As a result, the following equation was used in this study to deduct the amount of urban encroachment:

$$A_{\text{adjust}}(t)^k = \left(A(t)^U - A(0)^U \right) \times H_n^{k \to U}, \quad (4)$$

where $A_{\text{adjust}}(t)^k$ is the total area deducted from class k for year t, $A(t)^k$ is the original total area of class k for year t, U is urban land, n is the number of land-use types (excluding urban land-use), and $H_n^{k \to U}$ is the empirical proportion of land loss due to urban encroachment on land-use type k in a historical period ($\sum_n H_n^{k \to U} = 1$). It was estimated by using empirical land-use of 2000 and 2010 from MODIS Land Cover Type Product and the urban land-use produced by J. Chen et al. (2015; see Table 3).

To run the FLUS software, training data were collected from the 2010 MODIS land-use map: These formed the inputs used to train and validate the neural network. The neural network was trained for each of the seventeen regions separately. To avoid the overfitting problem, we trained the neural network with a small portion of the data but verified the model accuracy with all of the data. The number of training samples amounted to 0.1 percent of the total number of the cells in the region. We then calculated the mean square error (MSE) for all of the cells of each region for each land-use type. Stratified random sampling was carried out to distribute the training data across the seventeen world regions fairly (Congalton 1991; Li and Yeh 2000). The samples, which amounted to 0.1 percent of the whole data set, were randomly distributed to the six land-use classes in each region in the world. A total of 455,546 samples collected globally were used to train the FLUS model (Table 4). The log-sigmoid function was selected as the transfer function of the FLUS model, so that the values of estimated probabilities would fall within [0, 1] (Li and Yeh 2002). The MSE was used as the objective function in the back-propagation (BP) training process for the ANN. The training process was stopped when the MSE was less than 0.01. The best set of FLUS parameters was obtained in accordance with the least MSE value. This procedure was automatically completed by our GeoSOS-FLUS software, which is

Table 3. The value of $H_n^{k \to U}$ estimated from empirical land use change in 2000–2010

	Forest	Grassland	Farmland	Barren	Total
Loss (km^2)	19,790	54,791	112,990	13,424	200,995
$H_n^{k \to U}$ (Percentage)	0.10	0.27	0.56	0.07	1

an extension to our previous GeoSOS software (Li, Chen, et al. 2011; Li, Shi, et al. 2011; available for download at http://www.geosimulation.cn/flus.html).

Simulation and Analysis

This model was used to produce a 1-km global land-use change map for the period 2010 to 2100, calibrated at 2010 land-use data. First, aggregated LULC information for seventeen world regions from the IPCC SRES was obtained from the IMAGE module. The simulation was implemented for each of these world regions separately.

IMAGE is equipped with the IPCC SRES set of scenarios that were developed for the IPCC Third Assessment (IPCC 2001). Because of the uncertainty of future conditions, scenario-based simulation is often required for exploring particular trajectories of change in the status of ecological and anthropogenic systems (Hurtt et al. 2011). Our simulation was based on the aggregated projected land-use demands of seventeen regions, which was obtained from the four major scenarios taken from the IPCC SRES (Sleeter et al. 2012; Sohl et al. 2012). These scenarios were distributed along two axes (Figure 4): On the vertical axis, at one end, A was used to represent an economic emphasis and, at the other, B denotes an environmental emphasis; on the horizontal axis, 1 denotes a global orientation, and 2 denotes a regional orientation. Each of the scenarios specifies a different level of population growth, economic development, and other socioeconomic and environmental variables, which in turn determine their distribution on the two axes.

The SRES scenarios only provide the aggregated LULC information for seventeen world regions or LULC maps at a 30-min resolution (Strengers et al. 2004). We just used the aggregated LULC information

as the constraints for creating the global 1-km LUCC product. We first obtained the aggregated LULC information for seventeen world regions from the IPCC SRES to meet the land demands of the FLUS model (Figure 1). With the LULC map initialized in 2010, the FLUS model was then used to simulate multitype land-use dynamics at the global scale for the period from 2010 to 2100.

Figure 5 shows the projected areas for major LULC classes for the period from 2010 to 2100 for each of the four SRES scenarios. The areas of the various land categories were directly calculated by using the IMAGE module. Although each of the four scenarios began with the same initial values for aggregated farmland, aggregated grassland, and aggregated forest in 2010, these values experience a strong deviation over time between SRES scenarios. This deviation in the quantity of a given land-use class under a given scenario is a result of the varying economic and environmental initiatives built into the IPCC SRES scenarios.

Farmland is a major land-use type, the dynamics of which affect food production and ecological systems. The change in farmland area was found to vary radically among the four scenarios (Figure 5A). In Scenario A2, the emphasis on economic growth can be linked to associated population growth, a development that can be projected to result in increases in farmland area in the period from 2010 to 2100 to support that growth. This increase in farmland area occurs at the loss of natural landscapes—as such, both grassland and forest area experience substantial losses.

Scenario A1B sees a short-term increase in aggregate farmland during the period from 2040 to 2070, followed by a decrease thereafter. As a whole, Scenarios A1B and B2 maintain stable amounts of farmland for securing food production. Scenario B1

Table 4. Number of pixels of training data for building the Future Land-Use Simulation model, using stratified random sampling across seventeen world regions

Canada	Central America	East Asia	Eastern Africa	Eastern Europe	Former USSR
20,629	18,514	23,090	24,268	10,396	50,315
Japan	Middle East	Northern Africa	Oceania	OECD Europe	South America
6,732	12,268	10,743	45,071	25,316	62,861
South Asia	Southeast Asia	Southern Africa	United States	Western Africa	
13,455	23,046	14,728	58,146	44,285	

Note: OECD = Organisation for Economic Co-operation and Development.
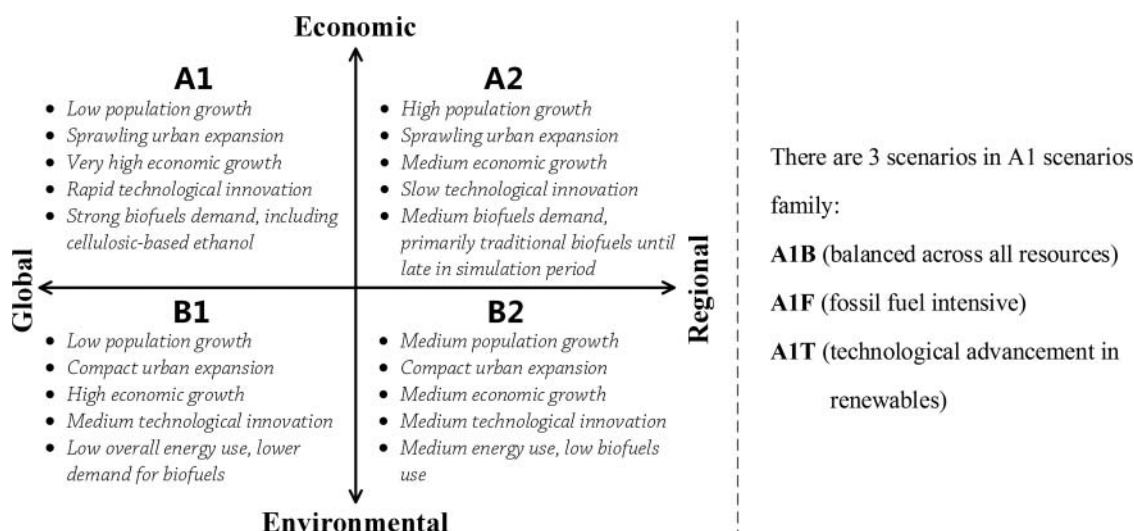
Figure 4. The settings of four major scenarios based on Intergovernmental Panel on Climate Change Special Report on Emission Scenarios (Sohl et al. 2012).

is quite different from the other scenarios, with substantial decreases seen in farmland area under these projected conditions. Overall, the Scenario A series projects greater increases in the aggregate area of farmland than the Scenario B series. In general, the Scenario 1 series witnesses smaller increases in the area of farmland than the Scenario 2 series.

Figure 5B depicts the future dynamics of areas of grassland at the global scale. Generally speaking, global grassland area can be expected to experience substantial losses in the future. Scenario B1 is the only exception to this, as some increases in grassland are predicted under these conditions. Scenario A2 witnesses the greatest decrease in the aggregate area of grassland globally.

Figure 5C shows future changes in the amount of forest under each of the four scenarios. Scenario B1 is projected to result in the greatest increase in the aggregate area of forest globally. In contrast, an obvious drop of forest area is observed under Scenario A2,

especially during the period from 2070 to 2100. Scenarios A1B and B2 share a similar pattern, both seeing a slight increase of forest area.

Our analysis reveals that the objectives of each of the scenarios was in fact reflected in the projection: The economically oriented scenarios attempt to maximize the amount of human-used land (e.g., farmland) and generally do so; the environmental-oriented scenarios aim to protect natural systems (e.g., grassland and forest) and also generally do so. These scenarios provide an important foundation for estimating the impacts of human activities on natural systems in a relatively uncertain future.

The proposed FLUS model was then used to simulate multitype land-use dynamics at a spatial resolution of 1 km for the period from 2010 to 2100. The development of a global 1-km land-use simulation method makes it possible to see how future urban land-use changes encroach on natural systems (e.g., reducing
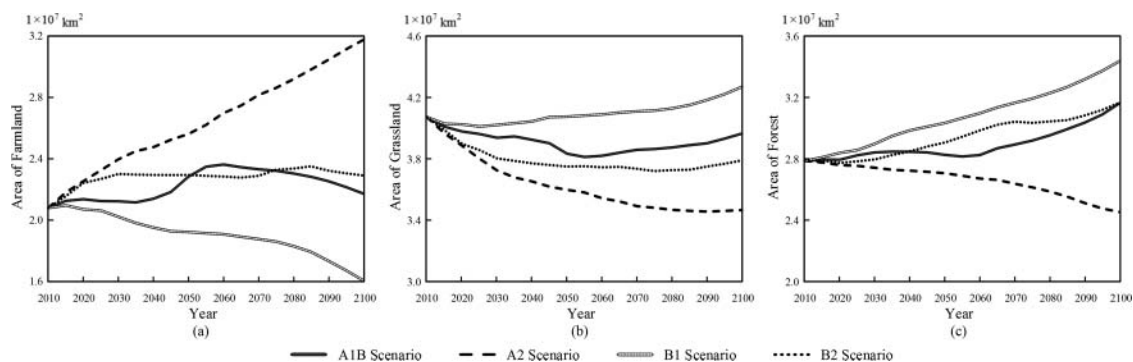
Figure 5. Projections of farmland area, grassland, and forest for 2010–2100, from the four Intergovernmental Panel on Climate Change Special Report on Emission Scenarios of IMAGE.

areas of grassland and forest) with adequate spatial detail for analysis. We implemented such a method using our own software, GeoSOS-FLUS (http://www.geosimulation.cn/flus.html). The whole set of 1-km FLUS product for the global land-use projection of years 2050 and 2100 can now be freely downloaded at http://geosimulation.cn/GlobalLUCCProduct.html. We selected a number of typical regions to illustrate the effects of using a finer resolution, because the global maps do not show the patterns clearly.

We used a transition percentage calculated as the amount of change (km^2) per grid cell (10 × 10 km^2) to represent land-use dynamics (Meiyappan et al. 2014). Figure 6 shows the transition percentage in farmland areas of a subregion in South America that is subject to intensive agricultural activity. Under the Scenario A series, aggregate farmland area undergoes a much greater percentage increase (evidenced in a greater number of sites that are marked dark green) than under the Scenario B series. In comparison, Scenario B1 projects decreasing percentages of farmland area (shown in red) in some locations.

Figure 7 depicts a subregion in North America that maintains a large percentage of grassland. Under the Scenario A series, this percentage undergoes more

visible reductions (shown as sites of dark red) than projected conditions under the Scenario B series. A particularly obvious reduction in grassland area is seen in the eastern part of the Great Plains of the United States; this change results from requirements for increased farmland that are built into this scenario. For the northern part of Mexico, Scenario A2 shows a large drop in the amount of grassland for a similar reason.

Figure 8 shows a typical region with concentrated forest in northeast Asia. Much greater decreases in the area of these forests are observed under the Scenario A series than the Scenario B series. The Scenario 1 series in turn leads to a greater increase in the area of forest in this subregion than that achieved under its counterpart, the Scenario 2 series. Japan, which is also shown in Figure 8, is quite different from adjacent landscapes, with decreasing areas of forest being projected under all four scenarios.

Figure 9 just shows the four scenarios of rapid growth of some Chinese cities from 2010 to 2050. This nation will continuously inherit intensified urban growth in the eastern part of the country, driven by its fast population increase and economic growth. Hot spots of urban growth patterns can be identified in the Bohai rim region, the North China Plain, the Yangtze
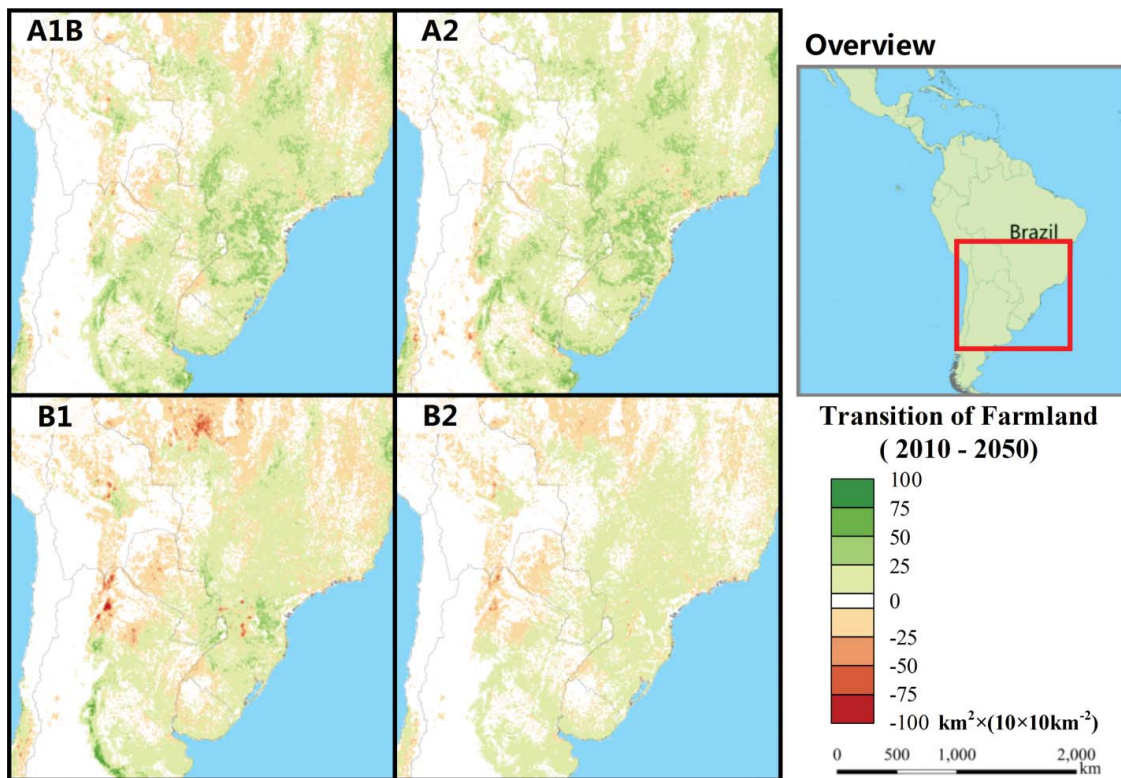
Figure 6. Changes (transition percentage) in the farmland area of a subregion in South America under four scenarios, 2010–2050. (Color figure available online.)

River Delta, and the Pearl River Delta. The simulation shows that the amounts of urban growth from more to less followed A2, A1B, B1, and B2. Especially with the focus on economic development, the Scenario A series will have a much larger amount of urban expansion than the Scenario B series.

## Model Validation and Simulation Performance Assessments

To validate this model, we calibrated the FLUS model again using the 2000 MODIS land-use map. We then simulated the changes from 2000 to 2010, at which point the model's simulated change was compared to the reference change during from 2000 to 2010. This allowed us to use the land-use data set of 2000 and 2010 for validating the accuracy of the FLUS model. So far the MODIS Land Cover Type Product seems to be the only available data for global land-use types. However, these MODIS data have a problem detecting urban land-use change because urban areas are almost kept unchanged in different years of these data. We rectified this problem by replacing the urban land use of MODIS with the urban land use produced by J. Chen et al. (2015) for the

years 2000 and 2010. J. Chen et al. (2015) created global land-use data for 2000 and 2010 based on the interpretation of 30-m resolution Landsat TM data. We only obtained the urban land use data, however, without other land-use types from their study. Without better validation data, the combination of these two data sets provides a feasible way for us to obtain the data for validating this improved land-use product.

We then used Figure of Merit (*FoM*) to measure the goodness of fit of the simulation for the land-use change from 2000 to 2010. The index of *FoM* is superior to the common kappa coefficient in the accuracy assessment of simulating changes (Pontius et al. 2008; Pontius, Peethambaram, and Castella 2011). This index can be mathematically expressed as the ratio of correct predicted change to the union of the observed change and predicted change (Pontius et al. 2008; Pontius, Peethambaram, and Castella 2011):

$$FoM = B/(A + B + C + D), \qquad (5)$$

where A is the area of error due to observed change predicted as persistence, B is the area correct due to observed change predicted as change, C is the area of
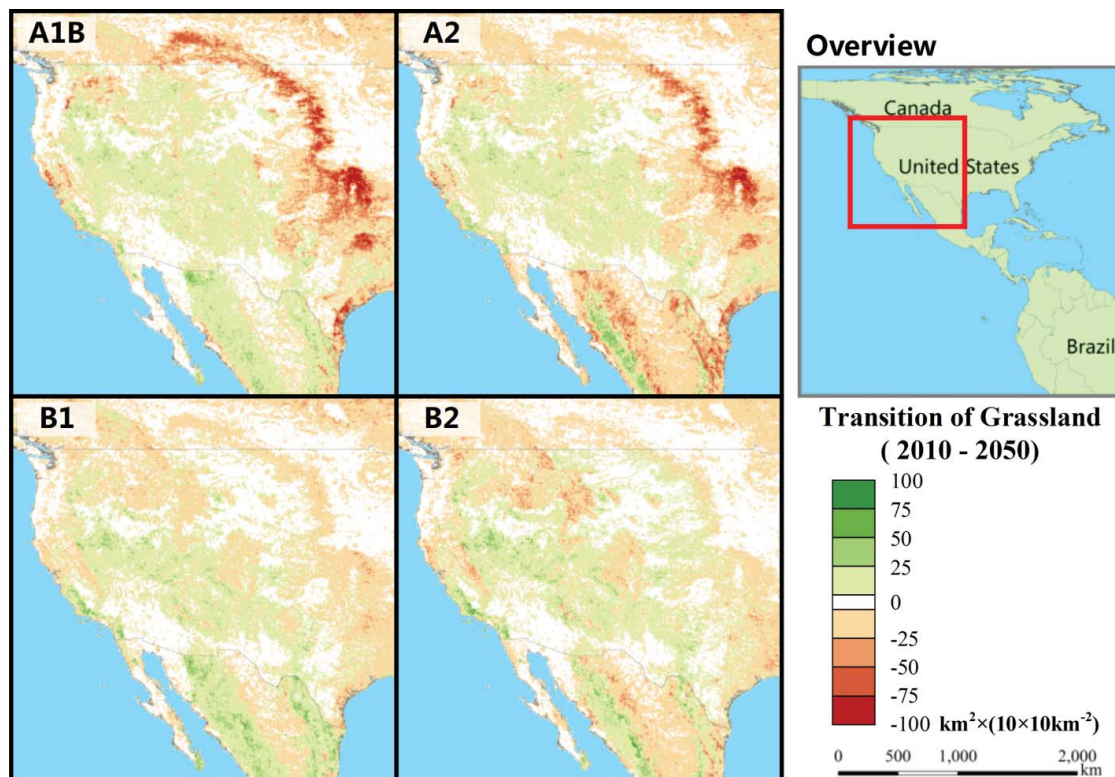
Figure 7. Changes (transition percentage) in the grassland area of a subregion in North America under four scenarios, 2010–2050. (Color figure available online.)
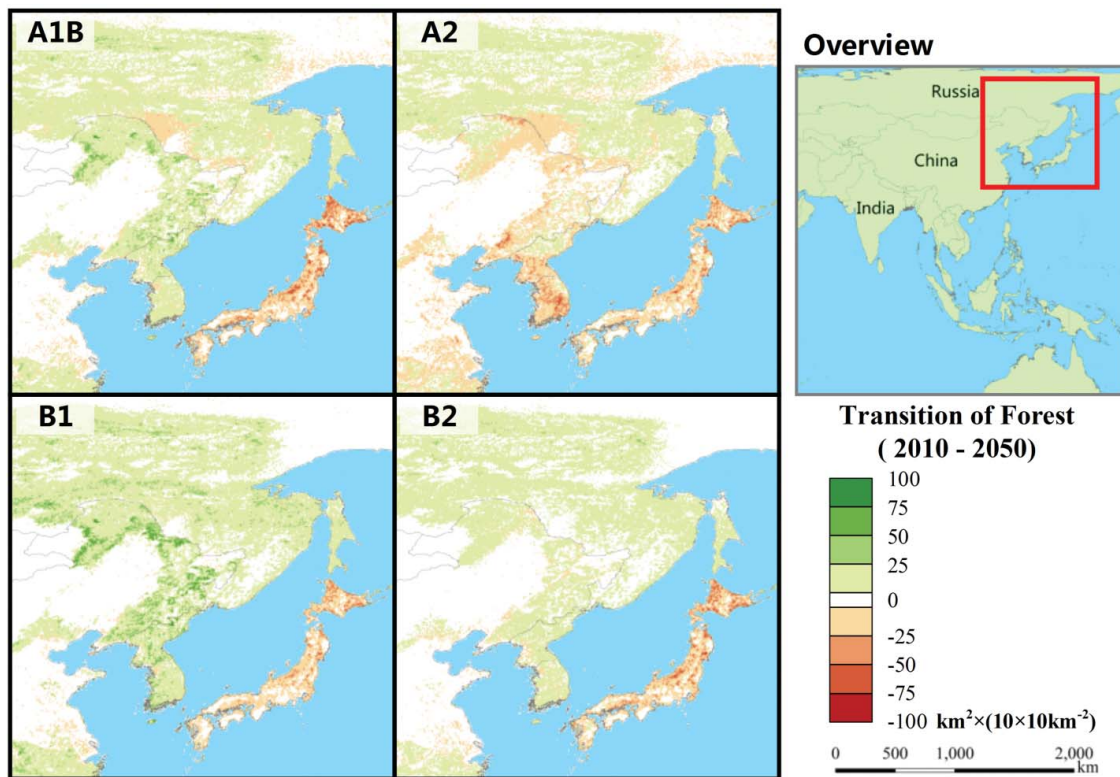
Figure 8. Changes (transition percentage) in the forest area of a subregion in northeast Asia under four scenarios, 2010–2050. (Color figure available online.)
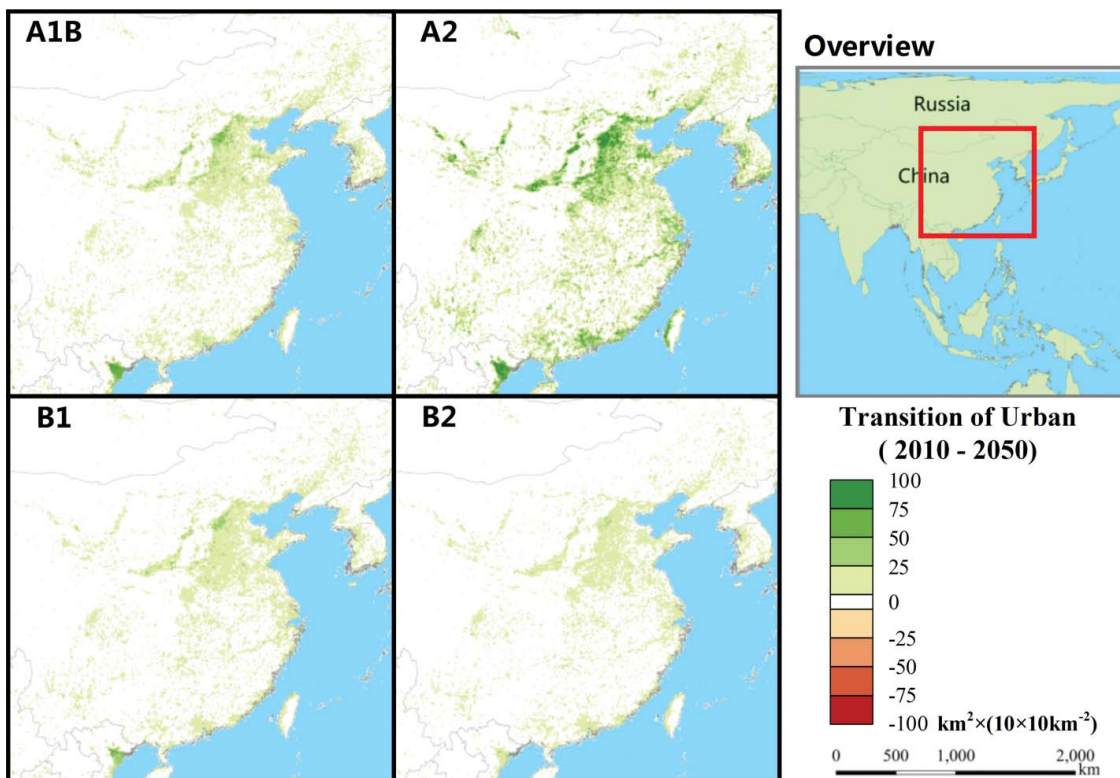

Figure 9. Changes (transition percentage) in the urban area in a part of China under four scenarios, 2010–2050. (Color figure available online.)

error due to observed change predicted as change to the wrong category, and D is the area of error due to observed persistence predicted as change.

Table 5 shows the values of *FoM* of the seventeen regions for the global land-use simulation from 2000 to 2010. The values of *FoM* of the seventeen regions range from 10 percent to 29 percent, with a mean of 19 percent. This indicates that the FLUS model in general has a range similar to the results of one of the other simulation studies. For example, the values of *FoM* range from 12 percent to 18 percent for modeling urban land-use dynamics in the study by Y. Chen et al. (2014). Pontius et al. (2008) also showed a range in *FoM* from 1 percent to 59 percent.

Urban dynamics constitute a major feature of land-use systems that cannot be ignored in environmental modeling. Many existing global land-use simulation models do not adequately represent urban features because of their coarse spatial resolutions. In response to this resolution problem, in this study we used the MODIS Land Cover Type Product (MCD12Q1) with a spatial resolution of 463 m for 2010 to quantify the effects of resolution downgrading on the representation of urban land-use patterns. For the comparison, the original resolution of MODIS was downgraded to 1 km and 10 km, respectively, to analyze the distortion of global urban area. Table 6 shows that the underestimation of global urban area was only 0.01 percent when the resolution was downgraded to 1 km but became 19.77 percent at the 10-km resolution, compared to the original 463-m MODIS land-cover product. This means that a 10-km resolution will cause a sizable distortion in representing urban land features.

The preceding analysis indicates that a 1-km resolution is much more accurate in preserving existing land-use patterns than a 10-km resolution or above. The use of coarse resolutions will also negatively affect the accuracy of simulations of future land-use patterns,

just as it does in relation to existing ones. We therefore also estimated the uncertainty present in simulating land-use change using a coarse resolution (e.g., 10-km). We evaluated the distortion of the urban area by overlaying 10 × 10 km grid cells over our simulated 1 × 1 km grid cells. A 10 × 10 km grid cell was counted as an urban cell if it contained a (simulated) urban area that was greater than 50 km^2 (or half of the area of a 10 × 10 km grid cell) in the 1-km resolution map. The results of this test are set out in Table 7. Findings indicate that between 60 percent and 97 percent of simulated urban growth that was visible in the 1-km resolution map was merged into other change classes in the 10-km resolution map for these four growth scenarios. It is obvious that a majority of actual urban growth will be lost using the 10-km resolution in undertaking land-use change simulation. Compared with existing products, therefore, this new 1-km product represents a far better option for maintaining urban features under an affordable computation burden.

Figure 10 compares the effects of using 1-km, 10-km, and 50-km resolutions for simulated land-use patterns in the major metropolitan areas around the world for Scenario A1B in 2050. A simple visual inspection clearly shows that global land-use maps with 10-km resolution or above will merge many small patches of urban land (shown in red in the figure) into other land-use classes, introducing a high level of uncertainty into global assessments.

We also carried out a visual inspection by comparing the consistency of the simulated land-use pattern generated by our model and that generated using IMAGE. Figure 11 shows the comparison of the simulated land-use patterns for Scenario A1B 2050 generated by our 1-km product (available at http://geosimulation.cn/GlobalLUCCProduct.html) and the IMAGE 30-min product (available at ftp://ftp.pbl.nl/image/public/Data/

Table 5. The values of Figure of Merit (%) of the seventeen regions for global land use simulation from 2000 to 2010

Canada	Central America	East Asia	Eastern Africa	Eastern Europe	Former USSR
10.11	23.17	28.25	19.81	10.63	15.98
Japan	Middle East	Northern Africa	Oceania	OECD Europe	South America
18.87	13.06	13.90	25.98	14.06	17.79
South Asia	Southeast Asia	Southern Africa	United States	Western Africa	
27.87	17.16	28.98	13.16	22.18	

Note: OECD = Organisation for Economic Co-operation and Development.

Table 6. Underestimation of global urban land area, using coarse resolutions based on MODIS Land Cover Type Product in 2010

	Spatial resolution		
	463 m	1 km	10 km
Global urban area (km^2)	656,360	656,437	526,600
Missing	—	0.01%	19.77%

SRES). It is clear that use of these two products has resulted in generally similar land-use patterns. The distribution of land-use types is consistent between them. A number of major distinctions can, however, be found between the modeling results of two products. First, our product provided a greater level of spatial detail (which is in turn crucial for identifying the spatial heterogeneity of land-use patterns). Second, a large number of urban clusters (shown in red) are missing in the results generated using the IMAGE product—these urban features are, in comparison, preserved in our 1-km product. This is particularly clear in the United States subregion, where small urban clusters can be recognized in the results gained through our model. It is almost impossible to maintain this small patch of urban areas using the well-known IMAGE product. The accurate representation of urban features is important, as urban systems contribute a major part of land-use dynamics.

This FLUS model is also targeted as a free land-use simulation tool for public use. It provides an affordable simulation for simulating global land-use change by general PCs. For example, our experiments were just carried out in a computer with 8 GB physical memory and Intel Core i7-4790 CPU (3.6 GHz). So far, the CLUE-S software package might be the best one that is available for land-use change simulation in the public domain (see http://www.ivm.vu.nl/en/Organisation/departments/spatial-analysis-decision-support/Clue/index.aspx). We found, however, that this

software cannot be used for simulating fine-scale global land-use change. If a raster image exceeds the size of 4,000 × 4,000, the computer will run out of the memory using the CLUE-S model. It is obvious that such a limitation cannot accommodate the needs of large-scale and high-resolution land-use/cover change simulation. Actually, the image size of the largest region, South America, reaches 7,778 × 8,082 for the 1-km resolution. This proposed FLUS model seems to have the capability to cope with the large-scale land-use simulation.

Discussion

Using CA methodology to simulate global land-use change, there might be a concern if the neighborhood relations of CA can still be suitable for resembling underlying processes and driving factors for global land-use change, given their long-term and global scales. Actually, the neighborhood effects have already been incorporated in other long-term simulation models, such as the regional-scale CA-based GEOMOD model (Estoque and Murayama 2012), continental-scale DynaCLUE model (Verburg and Overmars 2009), continental- and global-scale Landshift model (Schaldach et al. 2011), and global-scale CLUMondo model (van Asselen and Verburg 2013). Their studies have demonstrated the usefulness of CA for capturing the structural changes of global land-use patterns. CA can represent spatial interactions that are implemented in the immediate neighborhood or in the hierarchical structure of the neighborhood (over larger distances; White, Engelen, and Uljee 1997). Through iterations and updates, CA can adequately incorporate the mechanisms of spatial interactions and feedbacks between system elements (Clarke, Hoppen, and Gaydos 1997). The mechanisms are especially important for capturing complex and realistic urban dynamics. A very limited number of studies have attempted to establish multitype LUCC simulation models (e.g., ANN-CA and CLUE-S series models), but

Table 7. Underestimation of global urban growth by using coarse resolutions for various scenarios

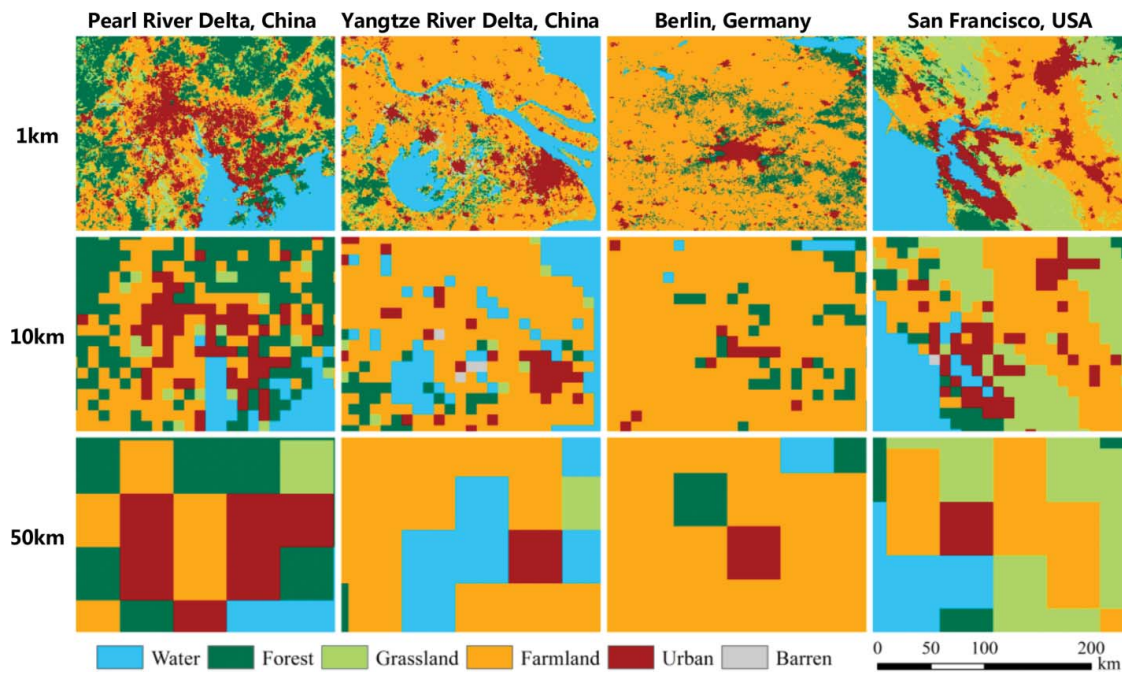|	Scenario			
2010–2050	A1B	A2	B1	B2
Simulated urban area at 1-km resolution (10^3 km^2)	817.6	1181.7	529.0	292.3
Simulated urban area at 10-km resolution (10^3 km^2)	232.6	465.9	64.8	8.0
Lost (%) by the 10-km resolution	71.55	60.57	87.75	97.26

Figure 10. Distortion of urban details for major metropolitan areas around the world for the year 2050, using 10-km and 50-km resolutions instead of a 1-km resolution. (Color figure available online.)
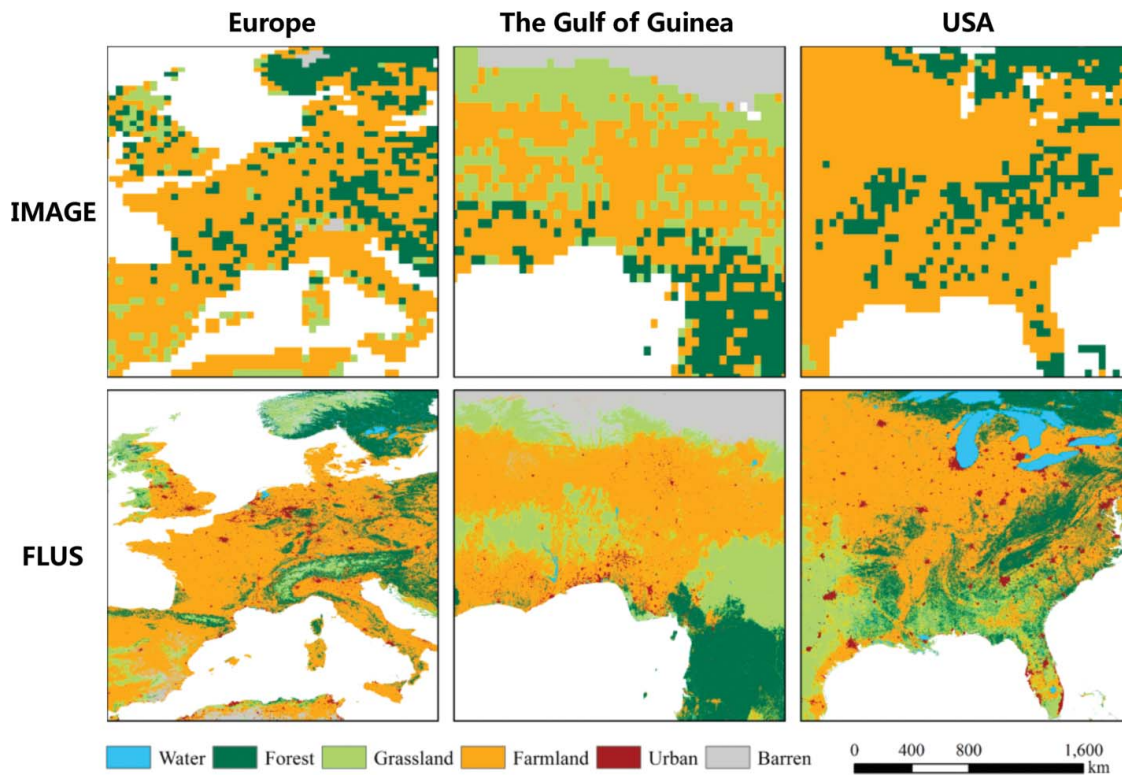

Figure 11. Improvement of spatial details of the 1-km product over the IMAGE 30-min product in the simulated land-use pattern in 2050 for Scenario A1B. (Color figure available online.)

these models have mainly been implemented at a regional scale to date (Li and Yeh 2002; Verburg et al. 2002; Verburg and Overmars 2009). Such models are also unable to deal with background climate changes, which in fact have profound effects in relation to landscape dynamics. These factors should be incorporated into long-term LUCC simulations under various human and climate effect scenarios.

Another issue with the implementation of fine-scale global land-use products is uncertainties and inconsistencies abound in using global driving data sets. These global driving factors that are processed and provided by different organizations or individuals are usually presented with various resolutions, ranging from 0.5 min (about 1 km on the equator) to 5 min (about 10 km on the equator). However, the resolutions of the variables used in our model are approximately equal to the 1-km resolution with the exception of the soil quality subdata set (Table 2). Even for the soil quality subdata set, the resolution of 5 min does not appear to be rough, compared with other driving factors. This is because the spatial heterogeneity of soil quality distribution is not as large as other driving factors such as population. The resolution of 5 min can have the assurance of capturing the actual distribution of soil quality.

So far our model is implemented using the projection of WGS_1984_Cylindrical_Equal_Area. Similarly, the LUSs model is also implemented in a raster resolution of 5 arc-min converted to equal area projection (Letourneau, Verburg, and Stehfest 2012). When using these models for the polar regions, a practical method is to transform the projections of the simulated land-use patterns to the sphere or other projections. A further improvement to the FLUS model is to implement it on a sphere when simulating land-use change for the entire globe. The use of a sphere can help reduce the shape distortions in the polar regions.

Conclusion

Climatic change analyses usually require long-term land-use simulation (e.g., over fifty years or longer) to assess the impacts of human activities on the Earth's system (Hurtt et al. 2011). This is the case in long-term scenario simulations of future carbon-climate projection (Moss et al. 2010). Through this study, we developed a spatially explicit LUCC model with much finer spatial resolution that can potentially be integrated with a variety of other models (e.g., hydrologic, climate, and biogeochemical models). Most existing global land-use change models, such as the IMAGE

model, provide scenario-based land-use projections at only a 30-min resolution (about 55-km resolution at the equator) according to the drivers of climate and macroeconomics. Recently, great efforts have been made to represent land-use dynamics at continental and global scales at a 5-min resolution (about 10-km resolution at the equator), resulting in, for instance, the LUSs model (Letourneau, Verburg, and Stehfest 2012) and the CLUMondo model (van Asselen and Verburg 2013). The 30-min IMAGE data, however, are the finest resolution available for public use at present. To our knowledge, the 1-km resolution FLUS product developed in this study constitutes the most spatially detailed technique for representing future LUCC in global environmental change assessments to date. The use of finer spatial resolution LUCC data can improve our ability to accurately model complex urban dynamics with more spatial details and thus understand the coupled human–environment systems. This new FLUS product results from integrating IMAGE with a CA model by incorporating the driving factors of demographics, global economics, energy production and consumption, and climate change.

Modeling land-use dynamics is a complex process: Socioeconomic and biophysical forces must be nested to understand and model land-use systems (Verburg et al. 2004). Because strict mathematical equations are difficult to define, land-use modeling can be facilitated using simulation models that work to disentangle those complex relationships. By implementing LUCC models at a global scale, simulation results can assist in change assessments relating to climate, biodiversity, and ecosystems, among others. Global land-use simulation is, however, itself difficult, involving great heterogeneity of geographical features and social settings among different regions in the world. The finer resolution simulation is dependent on the availability of corresponding high-quality drivers. Fortunately, most of the common global drivers are now available at 1-km resolution, which is crucial for guaranteeing the modeling of global land-use change.

This study has demonstrated that urban dynamics is an important component of land-use change. Various studies have indicated that changes of a few percent in the size of urban areas have the potential to affect ecological systems (Atkinson 2000; Schneider, Friedl, and Potere 2009). Unfortunately, the variable of urban area has been kept fixed in global models and land-use products like the IMAGE model and the MODIS product, either because such change information is simply lacking or because the spatial resolutions used

are too coarse to reflect this change. Ignoring urban dynamics builds a range of uncertainties into global environmental assessments. Although recent studies have made attempts to incorporate the urban growth component in their simulations, the use of coarse resolutions will severely reduce their effectiveness. As the tests undertaken in this study demonstrate, coarse resolutions produce major distortion in capturing and representing urban features.

This study has made a general improvement to the spatial resolution of global land-use simulation techniques. By converting the fine resolution data to coarser resolutions, we found that even the best resolution (10 km) used in a recent study will severely underreport global urban land area by an astounding 19.77 percent. We found that the 10-km global land-use product also underestimated 60 to 97 percent of simulated urban growth for the period from 2010 to 2050. Such biases can produce great uncertainty in global environmental assessment modeling because urban dynamics constitute a major component of land-use change. The model proposed here could greatly advance global land-use simulation by providing a more accurate way of modeling land-use change in global studies.

In future studies, the temporal resolution could be improved further so that land-use simulation models can be closely coupled with other environmental models. The feedback between land-use simulation models and these models should be considered at greater length to improve the performance of land-use simulations. A better set of validation data needs to be collected from satellite images for the validation of this new model.

Acknowledgments

Funding

ORCID

Xia Li http://orcid.org/0000-0003-3050-8529
Xiaoping Liu http://orcid.org/0000-0003-4242-5392

References

Atkinson, R. 2000. Atmospheric chemistry of VOCs and NOx. *Atmospheric Environment* 34 (12): 2063–2101.

Batty, M., and Y. Xie. 1994. From cells to cities. *Environment and Planning B: Planning and Design* 21 (7): S31–S48.

Chen, J., J. Chen, A. Liao, X. Cao, L. Chen, X. Chen, C. He, et al. 2015. Global land cover mapping at 30m resolution: A POK-based operational approach. *ISPRS Journal of Photogrammetry and Remote Sensing* 103:7–27.

Chen, Y., X. Li, X. Liu, and B. Ai. 2014. Modeling urban land-use dynamics in a fast developing city using the modified logistic cellular automaton with a patch-based simulation strategy. *International Journal of Geographical Information Science* 28 (2): 234–55.

Chen, Y., X. Li, X. Liu, B. Ai, and S. Li. 2016. Capturing the varying effects of driving forces over time for the simulation of urban growth by using survival analysis and cellular automata. *Landscape and Urban Planning* 152:59–71.

Clarke, K. C., and L. J. Gaydos. 1998. Loose-coupling a cellular automaton model and GIS: Long-term urban growth prediction for San Francisco and Washington/Baltimore. *International Journal of Geographical Information Science* 12 (7): 699–714.

Clarke, K. C., S. Hoppen, and L. Gaydos. 1997. A self-modifying cellular automaton model of historical urbanization in the San Francisco Bay area. *Environment and Planning B: Planning and Design* 24 (2): 247–61.

Congalton, R. G. 1991. A review of assessing the accuracy of classifications of remotely sensed data. *Remote Sensing of Environment* 37 (1): 35–46.

Estoque, R. C., and Y. Murayama. 2012. Examining the potential impact of land-use/cover changes on the ecosystem services of Baguio city, the Philippines: A scenario-based analysis. *Applied Geography* 35 (1–2): 316–26.

Fischer, G., F. Nachtergaele, S. Prieler, H. T. van Velthuizen, L. Verelst, and D. Wiberg. 2008. *Global agro-ecological zones assessment for agriculture (GAEZ 2008)*. Laxenburg, Austria, and Rome, Italy: IIASA and FAO. http://webarchive.iiasa.ac.at/Research/LUC/External-World-soil-database/HTML/SoilQuality.html?sb=10

Gregg, J. W., C. G. Jones, and T. E. Dawson. 2003. Urbanization effects on tree growth in the vicinity of New York City. *Nature* 424 (6945): 183–87.

Hijmans, R. J., S. E. Cameron, J. L. Parra, P. G. Jones, and A. Jarvis. 2005. Very high resolution interpolated climate surfaces for global land areas. *International Journal of Climatology* 25:1965–78.

Hurtt, G. C., L. P. Chini, S. Frolking, R. A. Betts, J. Feddema, G. Fischer, J. P. Fisk, et al. 2011. Harmonization of land-use scenarios for the period 1500–2100: 600 years of global gridded annual land-use transitions, wood harvest, and resulting secondary lands. *Climatic Change* 109 (1–2): 117–61.

Hurtt, G. C., S. Frolking, M. G. Fearon, B. Moore, E. Shev-liakova, S. Malyshev, S. W. Pacala, and R. A. Houghton. 2006. The underpinnings of land-use history: Three centuries of global gridded land-use transitions, wood-harvest activity, and resulting secondary lands. *Global Change Biology* 12 (7): 1208–29.

Intergovernmental Panel on Climate Change (IPCC). 2001. *Climate change 2001: Synthesis report: Third assessment report of the Intergovernmental Panel on Climate Change.* Cambridge, UK: Cambridge University Press.

Letourneau, A., P. H. Verburg, and E. Stehfest. 2012. A land-use systems approach to represent land-use dynamics at continental and global scales. *Environmental Modelling & Software* 33:61–79.

Li, X., Y. Chen, X. Liu, D. Li, and J. He. 2011. Concepts, methodologies, and tools of an integrated geographical simulation and optimization system. *International Journal of Geographical Information Science* 25 (4): 633–55.

Li, X., X. Shi, J. He, and X. Liu. 2011. Coupling simulation and optimization to solve planning problems in a fast-developing area. *Annals of the American Association of Geographers* 101 (5): 1032–48.

Li, X., and A. G. Yeh. 2000. Modelling sustainable urban development by the integration of constrained cellular automata and GIS. *International Journal of Geographical Information Science* 14 (2): 131–52.

———. 2002. Neural-network-based cellular automata for simulating multiple land-use changes using GIS. *International Journal of Geographical Information Science* 16 (4): 323–43.

———. 2004. Data mining of cellular automata's transition rules. *International Journal of Geographical Information Science* 18 (8): 723–44.

Liu, X., X. Li, X. Shi, S. Wu, and T. Liu. 2008. Simulating complex urban development using kernel-based non-linear cellular automata. *Ecological Modelling* 211 (1): 169–81.

Liu, X., X. Li, X. Shi, X. Zhang, and Y. Chen. 2010. Simulating land-use dynamics under planning policies by integrating artificial immune systems with cellular automata. *International Journal of Geographical Information Science* 24 (5): 783–802.

Liu, X., X. Liang, X. Xu, J. Ou, X. Li, Y. Chen, S. Li, S. Wang, and F. Pei. Forthcoming. An integrated model for simulating multiple land-use scenarios by coupling human and natural effects. *Landscape and Urban Planning.*

Liu, X., L. Ma, X. Li, B. Ai, S. Li, and Z. He. 2014. Simulating urban growth by integrating landscape expansion index (LEI) and cellular automata. *International Journal of Geographical Information Science* 28 (1): 148–63.

Meiyappan, P., M. Dalton, B. C. O Neill, and A. K. Jain. 2014. Spatial modeling of agricultural land-use change at global scale. *Ecological Modelling* 291:152–74.

Moss, R. H., J. A. Edmonds, K. A. Hibbard, M. R. Manning, S. K. Rose, D. P. Van Vuuren, T. R. Carter, et al. 2010. The next generation of scenarios for climate change research and assessment. *Nature* 463 (7282): 747–56.

Nakicenovic, N., and R. Swart. 2000. *IPCC special report on emissions scenarios.* Cambridge, UK: Cambridge University Press.

Pontius, R. G., Jr., W. Boersma, J. Castella, K. Clarke, T. de Nijs, C. Dietzel, Z. Duan, et al. 2008. Comparing the input, output, and validation maps for several models of land change. *The Annals of Regional Science* 42 (1): 11–37.

Pontius, R. G., S. Peethambaram, and J. Castella. 2011. Comparison of three maps at multiple resolutions: A case study of land change simulation in Cho Don District, Vietnam. *Annals of the Association of American Geographers* 101 (1): 45–62.

Santé, I., A. M. García, D. Miranda, and R. Crecente. 2010. Cellular automata models for the simulation of real-world urban processes: A review and analysis. *Landscape and Urban Planning* 96 (2): 108–22.

Schaldach, R., J. Alcamo, J. Koch, C. Kölking, D. M. Lapola, J. Schüngel, and J. A. Priess. 2011. An integrated approach to modelling land-use change on continental and global scales. *Environmental Modelling & Software* 26 (8): 1041–51.

Schneider, A., M. A. Friedl, and D. Potere. 2009. A new map of global urban extent from MODIS satellite data. *Environmental Research Letters* 4 (4): 44003.

Seto, K. C., B. Güneralp, and L. R. Hutyra. 2012. Global forecasts of urban expansion to 2030 and direct impacts on biodiversity and carbon pools. *Proceedings of the National Academy of Sciences* 109 (40): 16083–88.

Seto, K. C., and J. M. Shepherd. 2009. Global urban land-use trends and climate impacts. *Current Opinion in Environmental Sustainability* 1 (1): 89–95.

Sleeter, B. M., T. L. Sohl, M. A. Bouchard, R. R. Reker, C. E. Soulard, W. Acevedo, G. E. Griffith, et al. 2012. Scenarios of land-use and land cover change in the conterminous United States: Utilizing the special report on emission scenarios at ecoregional scales. *Global Environmental Change* 22 (4): 896–914.

Soares-Filho, B. S., D. C. Nepstad, L. M. Curran, G. C. Cerqueira, R. A. Garcia, C. A. Ramos, E. Voll, A. McDonald, P. Lefebvre, and P. Schlesinger. 2006. Modelling conservation in the Amazon basin. *Nature* 440 (7083): 520–23.

Sohl, T., and K. Sayler. 2008. Using the FORE-SCE model to project land-cover change in the southeastern United States. *Ecological Modelling* 219 (1): 49–65.

Sohl, T. L., B. M. Sleeter, K. L. Sayler, M. A. Bouchard, R. R. Reker, S. L. Bennett, R. R. Sleeter, R. L. Kanengieter, and Z. Zhu. 2012. Spatially explicit land-use and land-cover scenarios for the Great Plains of the United States. *Agriculture, Ecosystems & Environment* 153:1–15.

Strengers, B., R. Leemans, B. Eickhout, B. de Vries, and L. Bouwman. 2004. The land-use projections and resulting emissions in the IPCC SRES scenarios as simulated by the IMAGE 2.2 model. *GeoJournal* 61 (4): 381–93.

United Nations, Department of Economic and Social Affairs, Population Division. 2014. *World urbanization prospects: The 2014 revision.* CD-ROM edition. New York: United Nations.

van Asselen, S., and P. H. Verburg. 2013. Land cover change or land-use intensification: Simulating land system change with a global-scale land change model. *Global Change Biology* 19 (12): 3648–67.

Verburg, P. H., and K. P. Overmars. 2009. Combining top-down and bottom-up dynamics in land-use modeling: Exploring the future of abandoned farmlands in Europe

with the Dyna-CLUE model. *Landscape Ecology* 24 (9): 1167–81.

Verburg, P. H., P. P. Schot, M. J. Dijst, and A. Veldkamp. 2004. Land use change modelling: Current practice and research priorities. *GeoJournal* 61 (4): 309–24.

Verburg, P. H., C. J. E. Schulp, N. Witte, and A. Veldkamp. 2006. Downscaling of land-use change scenarios to assess the dynamics of European landscapes. *Agriculture, Ecosystems & Environment* 114 (1): 39–56.

Verburg, P. H., W. Soepboer, A. Veldkamp, R. Limpiada, V. Espaldon, and S. S. Mastura. 2002. Modeling the spatial dynamics of regional land-use: The CLUE-S model. *Environmental Management* 30 (3): 391–405.

Verburg, P. H., S. van Asselen, E. H. van der Zanden, and E. Stehfest. 2013. The representation of landscapes in global scale assessments of environmental change. *Landscape Ecology* 28 (6): 1067–80.

White, R., G. Engelen, and I. Uljee. 1997. The use of constrained cellular automata for high-resolution modelling of urban land-use dynamics. *Environment and Planning B: Planning and Design* 24 (3): 323–43.

Wu, F. 2002. Calibration of stochastic cellular automata: The application to rural–urban land conversions. *International Journal of Geographical Information Science* 16 (8): 795–818.

Zuidema, G., G. J. van den Born, J. Alcamo, and G. Kreileman. 1994. Simulating changes in global land cover as affected by economic and climatic factors. *Water, Air, and Soil Pollution* 76 (1–2): 163–98.

XIA LI is a Yat-sen Chair Professor in the School of Geography and Planning, Sun Yat-sen University, Guangzhou 510275, P.R. China. E-mail: lixia@mail.sysu.edu.cn. His research interests include urban expansion, land-use planning, and land-use simulation and optimization.

GUANGZHAO CHEN is a PhD Candidate in the School of Geography and Planning, Sun Yat-sen University, Guangzhou 510275, P.R. China. E-mail: chengzh7@mail2.sysu.edu.cn. His research interests include land-use simulation, urban expansion, big data, and land-use classification.

XIAOPING LIU is a Professor in the School of Geography and Planning, Sun Yat-sen University, Guangzhou 510275, P.R. China. E-mail: liuxp3@mail.sysu.edu.cn. His research interests include land-use planning, urban expansion, big data, and land-use simulation.

XUN LIANG is a PhD Candidate in the School of Geography and Planning, Sun Yat-sen University, Guangzhou 510275, P.R. China. E-mail: liangxunnice@foxmail.com. His research interests include land-use simulation and optimization, urban expansion, and land-use planning.

SHAOJIAN WANG is a Lecturer in the School of Geography and Planning, Sun Yat-sen University, Guangzhou 510275, P.R. China. E-mail: 1987wangshaojian@163.com. His research interests include urbanization, environmental changes, and economic geography.

YIMIN CHEN is a Lecturer in the School of Geography and Planning, Sun Yat-sen University, Guangzhou 510275, P.R. China. E-mail: chenym49@mail.sysu.edu.cn. His research interests include land-use planning, urban expansion, big data, and land-use simulation.

FENGSONG PEI is an Associate Professor at Jiangsu Normal University, Xuzhou 221116, P.R. China. E-mail: peifs@foxmail.com. His research interests include environmental remote sensing and land-use and land-cover simulation.

XIAOCONG XU is a PhD Candidate in the School of Geography and Planning, Sun Yat-sen University, Guangzhou 510275, P.R. China. E-mail: xuxiaoc@mail3.sysu.edu.cn. His research interests include environmental changes, snow cover estimation, and remote sensing image processing.